Performance-based slenderness limits for deformations and crack control of reinforced concrete flexural members

Antonio Marí[1], Lluís Torres[2], Eva Oller[1], Cristina Barris[2]

[1] Dept. of Civil and Environmental Engineering. Technical University of Catalonia (UPC), Barcelona, Spain

[2] Dept. of Mechanical Engineering and Industrial Construction. University of Girona (UdG), Girona, Spain

ABSTRACT

The use of high strength materials allows flexural members to resist the design loads or to cover long spans with a reduced depth. However, the strict cross section dimensions and reinforcement amount required in ULS are often insufficient to satisfy the serviceability limit states. Due to the complexity associated to a rigorous computation of deflections and cracks width in cracked RC members along their service life, an effective way to ensure the satisfaction of the SLS is to limit the slenderness ratio *l/d* of the element. In the present study, the slenderness limit concept, previously used for deflection control, is generalized to incorporate the crack width limitations in the framework of structural performance-based design. Equations for slenderness limits incorporating the main parameters influencing the service behaviour of RC members are derived. Cracking and long-term effects are accounted for through simplified coefficients derived from structural concrete mechanics and experimental observations. The proposed slenderness limits are compared with those derived from a numerical non-linear time-dependent analysis for two case studies, and also with those obtained using the EC2 procedure for deflection calculation in terms of constant applied load and constant reinforcement strain. Very good results have been obtained in terms of low errors and scatter, showing that the proposed slenderness limits are a useful tool for performance-based design of RC structures.

Keywords: Slenderness limits, deflection, crack width, Serviceability Limit State, reinforced concrete, reinforcement ratio, performance-based design

1. INTRODUCTION

Excessive deformations may cause damage to non-structural elements, as well as problems related to aesthetics or functionality on Reinforced Concrete (RC) structures. The use of high strength materials may allow reductions in the depth of flexural elements or increments of their span length for strength requirements but, at the same time, may drive to a considerable increment of deflections and cracks width.

To avoid excessive deflections that affect the serviceability performance of the structural members, their allowable design value is limited to a fraction of their span *l*. For instance, a limit of *l*/250 is indicated in the Eurocode 2 [1] or in the fib Model Code for Concrete Structures 2010 [2] for the deflection due to quasi-permanent loads. Likewise, a limit of *l*/500 is applicable for the increment of deflection after construction of partitions or other elements susceptible to damage. Other limits may also be considered, according to the nature and sensitivity of the elements to be supported.

Actual deflections may considerably differ from computed values due to the complex phenomena affecting the service behaviour of RC structures, mainly cracking, creep and shrinkage of concrete, and to the uncertainty associated with some governing parameters such as the concrete tensile strength. Furthermore, long-term deflections may be significant with respect to the instantaneous ones and are influenced by environmental conditions, element dimensions, concrete properties, reinforcement ratios, construction sequence, value and duration of sustained loading and age at loading.

Due to the complexity associated with a rigorous calculation of deflections, there has been a concern in providing practical methods aimed at considering, in a simplified way, the influence of cracking and the long-term effects, which have been included in several codes and recommendations (ACI 318 [3], CEB manual on cracking and deformations 1985 [4], Eurocode 2 [1], MC2010 [2]). Even so, there is an extensive literature about discussion, improvement, or

54 further simplification of such simplified methods (Gilbert [5], Bischoff and Scalon [6], Mari et al.
55 [7], Gribniak et al. [8]).
56 Due to the uncertainties existing in the estimation of deflections, one of the most practical and
57 effective ways to control excessive deflections is to provide the element with sufficient stiffness,
58 which can be achieved by limiting the slenderness ratio, *l*/*d*, of the element. Furthermore, a proper
59 selection of *l*/*d* may help in providing an adequate sizing of the cross section from the first steps of
60 the design process thus contributing to its simplification.
61 Different proposals and studies about limit slenderness ratios to avoid excessive deflections have
62 been previously carried out. Among them, Rangan [9] developed, in 1982, allowable span-to-depth
63 ratios for RC beams and one-way slabs based on Branson's method for computation of deflections
64 (ACI 318-77 [10]) in which the main parameters were explicitly introduced to obtain an expression
65 of *l*/*d* dependent on the applied loads. This proposal was adapted by Gilbert [11] to RC slabs with
66 different construction and support conditions by introducing a coefficient based on an extensive
67 series of parametric computer experiments. A similar expression was developed by Scanlon and
68 Choi [12] as an alternative to values in ACI 318-95 [13]. A comparative study was carried out to
69 assess the limitations of tabulated values in the code and provide a more general and explicit
70 approach. Some other comparative studies were performed by Lee and Scanlon [14], who analyzed
71 proposals from different codes (ACI 318-08 [15], BS 8110-1:1997 [16], Eurocode 2 [1], and AS
72 3600-2001 [17]) and a more refined equation was proposed by Scanlon and Lee [18]. Although the
73 study was focused on the performance of slenderness limits in ACI 318, it evidenced that proposals
74 from different recognized codes did not always provide the same results, due to the combined
75 effect of the assumptions made in the equations and the simplifications introduced for a more
76 practical use of the slenderness ratios.
77 Bischoff and Scanlon [19] developed slenderness limits equations to satisfy deflection and strength
78 requirements for RC one-way slabs and beams, presented as a function of the reinforcement ratio
79 and the deflection-to-span limit. Deflections based on Bischoff's approach [20] for equivalent
80 moment of inertia and a long-term deflection multiplier from ACI318 were considered. The
81 maximum flexural capacity of the member was taken into account. A study to assess the effects of

the main parameters, as well as a comparative analysis with values given in ACI318 was carried out. Results showed that members satisfying the ACI minimum thickness requirements did not necessarily comply with the deflection limits prescribed by ACI 318.

Pérez Caldentey et al. [21] proposed a simplified formulation for slenderness limits based on EC2 approach for deflection calculation to improve the lack of physical basis for the slenderness limits provided in the current version of EC2 [1]. The formulation was based on maximum flexural capacity of the member and included the effect of live load to total load ratio, the possibility of using different limits of maximum deflection and a generalization of a factor accounting for different support conditions.

Gardner [22] performed a comparative study among proposals of slenderness limits from different codes and authors. The influence of different parameters was discussed, such as the level of load assumed. Differences among methods were attributed to the effect of the different assumptions and simplifications made.

Control of cracking is another important aspect related to serviceability behavior of RC structures. Different parameters may influence crack width, but it is widely accepted that it is directly related to the tensile reinforcement strain (EC2 [1], MC2010 [2], Balázs and Borosnyoi [23], Pérez-Caldentey et al [24], Gergely and Lutz [25], Frosch [26]). Strains (or stresses) in the tensile reinforcement can be calculated from the flexural moment distribution and sectional mechanical properties, and slenderness limits (as it is seen in the paper) related to a maximum stress in the reinforcement can be obtained. As a consequence, limitations of deflections may be related to the limitations of the cracks width required for aesthetic and durability reasons. From the above considerations it can be said that it may be possible to find a domain of solutions in terms of l/d, reinforcement ratio and reinforcement stress or strain, which allow the simultaneous fulfilment of the SLS and the ULS of flexure.

Barris et al. [27] studied the application of EC2 [1] formulation on SLS to Fiber Reinforced Polymer (FRP) RC flexural members, obtaining a formulation to determine the slenderness limits that comply with the deflection limitation, maximum crack width and stresses in materials,

109 considering the principles of equilibrium and strain compatibility (plane sections remaining plane
110 after bending) and linear elastic behavior of materials.
111 From the analysis of the existing literature, it is seen that although many relevant works have been
112 carried out on the subject of slenderness limits for deflection control, so far there is not a unique
113 accepted model to estimate the l/d ratio. It has been observed that some models do not allow to
114 follow easily the rational basis for their application, others do not incorporate explicitly creep and
115 shrinkage strains for estimating long-term deflections (for instance those based on the simplified
116 approach of ACI 318), and others are based on the maximum flexural capacity of the member, thus
117 initially providing more strict values than those needed for the actual loads. Furthermore, the
118 simultaneous fulfilment of a limit of stress intended for control of cracking is not taken into
119 consideration.
120 In this study, the slenderness limit concept for deflection control is generalized to incorporate the
121 crack width limitations in the framework of structural performance-based design. Based on the
122 deflection calculation methodology proposed in EC2 [1] (MC2010 [2]), equations for slenderness
123 limits incorporating the main influencing parameters are derived. Cracking and long-term effects
124 are accounted for through simplified coefficients derived from the mechanical principles and
125 experimental observations of RC sections. Slenderness limits obtained with the proposed procedure
126 are compared in case studies with results from a numerical non-linear time-dependent analysis, as
127 well as with slenderness ratios obtained using the EC2 [1] procedure for deflection calculation in
128 terms of constant applied load and constant reinforcement strain.
129

130 ## 2. SLENDERNESS RATIO ASSOCIATED TO DEFLECTION LIMITS

131 ### 2.1. General

132 Consider a beam subjected to a dead load (g) and live load (q), uniformly distributed along the span
133 length, so that the total load is $p = g + q$. Being ψ_2 the factor for the quasi-permanent load
134 combination, the ratio between the quasi-permanent load and the total load, k_g, is defined as:

135 $$k_g = \frac{g + \psi_2 q}{g + q} \quad (1)$$

The long-term deflection (including instantaneous and time-dependent deflections) produced by the quasi-permanent load combination must be limited to a fraction of the span length ($a_{qp} < l/C$) [1]:

$$a_{qp} = k_b \frac{k_g p l^4 k_t}{E_c I_{eff}} \leq \frac{l}{C} \tag{2}$$

where p is the total characteristic load ($g + q$); $k_g \cdot p$ is the quasi-permanent load; k_t is a factor that relates the time-dependent to the instantaneous deflection due to quasi-permanent loads; k_b is a factor to account for the support conditions (i.e. $k_b = 5/384$ for simply supported members); l is the span length; C is a constant that indicates the fraction of the length for limitation of deflections (i.e., $C = 250$ for the long-term deflection under the quasi-permanent load combination); I_{eff} is the effective moment of inertia, which takes into account concrete cracking and tension stiffening; and E_c is the modulus of elasticity of concrete.

In the next sections, each term of Eq. (2) will be derived and a simplified expression for the deflection slenderness limit will be obtained.

2.2. Effective moment of inertia I_{eff} and cracking factor k_r

In the present study, it is considered that the members are cracked under the quasi-permanent load combination, assuming that they could have been subject to the characteristic load, i.e. the maximum possible service load, since otherwise the deflections would be much lower than those associated to the limit state of deflection. However, parts of the members may be not cracked (near the zero bending moment regions) and, in addition, the concrete surrounding the reinforcement, placed between cracks contributes to the stiffness of the cracked regions. Therefore, an effective moment of inertia of the cracked section, I_{eff}, should be used for deflection calculations accounting for cracking and tension stiffening. Such effective moment of inertia can be derived from the bilinear interpolation method for calculation of instantaneous deflections, as provided by the MC2010 [2]:

$$I_{eff} = \frac{I_I I_{II}}{I_I \zeta + I_{II}(1-\zeta)} = \frac{I_{II}}{\zeta + \frac{I_{II}}{I_I}(1-\zeta)} \tag{3}$$

where I_I and I_{II} are, respectively, the moments of inertia of the uncracked and the fully cracked sections and ζ is an interpolation coefficient, which depends on the type of load and level of cracking, given by:

$$\zeta = 1-\beta\left(\frac{\sigma_{sr}}{\sigma_s}\right)^2 \cong 1-\beta\left(\frac{M_{cr}}{M_a}\right)^2 \tag{4}$$

where β is a coefficient accounting for the type of loading (β = 0.5 for repeated or sustained loads); σ_{sr} is the stress in the tension reinforcement calculated on the basis of a cracked section under the bending moment M_{cr} that cause first cracking and σ_s is the maximum attained stress in the tension reinforcement calculated on the basis of a cracked section under the load considered which produces a bending moment M_a in the section studied.

The uncracked and fully cracked moments of inertia for a rectangular section of width *b*, effective depth *d* and total depth *h* can be obtained, neglecting the contribution of the compression reinforcement, by using the following equations:

$$I_I = I_g = \frac{bh^3}{12} \tag{5}$$

$$I_{II} = bd^3 n\rho\left(1-\frac{x}{d}\right)\left(1-\frac{x}{3d}\right) \tag{6}$$

where: $\rho = A_s/(bd)$ is the tensile reinforcement ratio; $n = E_s/E_c$ is the modular ratio between reinforcement and concrete; *x* is the neutral axis depth of the fully cracked section which can be estimated, neglecting the contribution of the compression reinforcement, as follows:

$$\frac{x}{d} = n\rho\left(1+\sqrt{1+\frac{2}{n\rho}}\right) \cong 0.75(n\rho)^{\frac{1}{3}} \tag{7}$$

By substituting Eqs. (5) and (6) into Eq. (3) the following non-dimensional expression for the non-dimensional effective moment of inertia $k_{rs} = I_{eff}/bd^3$ is obtained:

$$k_{rs} = \frac{I_{eff}}{bd^3} = \frac{n\rho\left(1-\frac{x}{d}\right)\left(1-\frac{x}{3d}\right)}{\zeta + 12\left(\frac{d}{h}\right)^3 n\rho\left(1-\frac{x}{d}\right)\left(1-\frac{x}{3d}\right)(1-\zeta)} \tag{8}$$

It can be seen that the non-dimensional effective moment of inertia depends on the homogenized reinforcement ratio $n\rho$, on the ratio between the effective and the total depth of the section d/h and on the ratio between the cracking moment and the maximum applied moment at the considered section, M_{cr}/M_a. The influence of the concrete mechanical properties is incorporated through the modular ratio $n = E_s/E_c$ and through the cracking moment $M_{cr} = bh^2 \cdot f_{ct,m}/6$.

In order to derive a simplified expression for the effective moment of inertia, a parametric study has been performed aimed to determine the influence of the above-mentioned parameters on k_{rs}. The following ranges of the above parameters have been covered: reinforcement ratios from ρ = 0.005 until ρ = 0.02, concrete strengths from 25 N/mm^2 to 50 N/mm^2 and steel stresses from 200 N/mm^2 to 300 N/mm^2, so that the value of M_{cr}/M_a ranges from 0.10 to 0.90. The result of such study for a total of 215 valid cases ($M_{cr} < M$), is shown graphically in Figure 1 where the value of k_{rs} is plotted as a function of $n\rho$.

Figure 1

It can be observed that k_{rs} depends almost linearly on $n\rho$. The mean value of the ratio between the linear approach of k_{rs} deduced from Figure 1 and the theoretical value is 1.01, and the coefficient of variation is 0.036. The maximum errors take place for very low reinforcement ratios, where the tension stiffening is relevant. Except for two cases with $M_{cr}/M > 0.87$, the maximum error found is 12%. Such good precision and low scatter indicate that the influence on k_{rs} of h/d, f_c and M_{cr}/M, is very small. Then, the following expression for k_{rs} and for the effective moment of inertia will be adopted in this work:

$$k_{rs} = 0.0125\left(1+36n\rho\right) \tag{9}$$

$$I_{eff} = k_{rs} bd^3 = 0.0125\left(1+36n\rho\right) bd^3 \tag{10}$$

The above effective moment of inertia is associated to a section, however, when computing deflections in a beam, a member effective moment of inertia must be evaluated, so the longitudinal

distribution of the reinforcement and the section geometry must be considered. For this reason, a mean member effective moment of inertia is adopted as follows:

$$I_{eff,m} = I_{eff,a}\frac{l_a}{l} + I_{eff,b}\frac{l_b}{l} + I_{eff,c}\frac{l_c}{l} \quad (11)$$

where $I_{eff,a}$, $I_{eff,b}$, and $I_{eff,c}$ are the effective moments of inertia at the two member ends A, B and at the center span C, respectively, while l_a, l_b and l_c are the respective lengths, as indicated by Figure 2.

Figure 2

In the case of simply supported beams, the effective moment of inertia of the center span section provides a good approximation of the member stiffness while, in the case of cantilevers, the effective moment of inertia of the fixed end section can be adopted. In both cases, the member is subjected to single curvature, without inversion of the bending moment sign. In continuous beams, however, the effective moment of inertia of both ends and center span affect the deflections and, therefore, l_a, l_b and l_c, must be adequately estimated. In absence of more accurate data, the following conservative values can be adopted: for members supported at one end and fixed at the other, and for end spans of continuous beams, $l_a/l = 0.20$ and $l_b/l = 0.80$; For members with both ends fixed, $l_a/l = l_b/l = 0.10$, and $l_c/l = 0.80$ and for interior spans of continuous beams $l_a/l = l_b/l = 0.15$, and $l_c/l = 0.70$.

In addition, in continuous members a change of sign of the bending moment takes place. Thus, in beams with non-symmetric cross section with respect to the principal axis of inertia, as T-sections, a different width of the uncracked zone must be considered at member ends A, B and at the center span, C.

In order to obtain a slenderness ratio, an equivalent member factor k_r should be derived. For this reason the effective moments of inertia $I_{eff,a}$, $I_{eff,b}$, and $I_{eff,c}$ are expressed in accordance to Eq. (10) and substituted in Eq. (11), providing the following expression for the global factor member k_r:

$$k_r = k_{rs,a}\frac{l_a}{l}\frac{b_a}{b_c} + k_{rs,b}\frac{l_b}{l}\frac{b_b}{b_c} + k_{rs,c}\frac{l_c}{l} \quad (12)$$

where $k_{rs,a}$, $k_{rs,b}$, and $k_{rs,c}$ are obtained from Eq. (9), using their respective reinforcement ratios ρ_a, ρ_b and ρ_c, and b_a, b_b and b_c are the width of the uncracked compressed concrete at sections A, B and C, respectively, so that when $l_a = 0$ and $l_b = 0$, $k_r = k_{rs,c}$.

2.3 Time-dependent deflections factor k_t

In order to obtain the increment of deflections due to creep and shrinkage, a time-dependent analysis of a cracked section subjected to a sustained load must be done. Due to the constraint produced by the steel to the increment of concrete strains along the time, a relaxation of the maximum compressive stress in concrete and an increment of the neutral axis depth and of the stresses in the compressive reinforcement take place. Furthermore, according to experimental observations, the strain at the tensile reinforcement is almost constant along the time, so the section can be assumed to rotate around the reinforcement, see Fig. 3 (Clarke et al [28], Murcia [29], Marí et al. [7]). This fact allows a simplification of the time-dependent sectional analysis, with very small errors if the reinforcement strain is considered constant along the time.

Figure 3

Adopting the above assumption, a time-dependent sectional analysis has been performed, which is presented in Annex 1, in which the time-dependent increment of curvature $\Delta\psi$ has been obtained. For this purpose, the equilibrium of forces in the section at any time has been set, compatibility of strain increments according to a planar deformation has been assumed, and the Age Adjusted Effective Modulus Method (AAEMM, Bazant [30]) has been used to account for ageing and obtain the creep produced under variable stresses. Thus, factor k_t of Eq. (2) that incorporates the time dependent effects when calculating the deflections, is given by Eq (13):

$$k_t = 1 + \frac{0.24\varphi + 1000\varepsilon_{cs}}{1 + 12n\rho'} \quad (13)$$

where φ is the creep coefficient at time $t \geq t_0$, ε_{cs} is the shrinkage strain, and $\rho' = A_s'/bd$ is the

compression reinforcement ratio. For continuous beams, where the compression reinforcement ratio varies along the element length, the following mean factor k_t is proposed:

$$k_t = k_{t,a}\frac{l_a}{l} + k_{t,b}\frac{l_b}{l} + k_{t,c}\frac{l_c}{l} \quad (14)$$

2.3. Slenderness associated to deflection limitation

Substituting Eq. (8) into Eq. (2), and after some arrangements, the following expression for the deflection slenderness limit, *l/d*, is derived:

$$\frac{l}{d} \le \sqrt[3]{\frac{E_c k_r}{C k_b k_g k_t \frac{p}{b}}} \quad (15)$$

where p is the characteristic uniformly distributed load per unit length; b is the beam width and p/b is the characteristic load applied by unit surface. Analyzing Eq. (15), some conclusions can be drawn: 1) the slenderness ratio l/d is lower for beams than for slabs because p/b is higher in the case of beams; 2) the higher the tensile and the compressive reinforcement ratios, the higher l/d, for the same load p/b, since k_r monotonically increases with ρ and k_t decreases when ρ' increases; 3) the higher the support constraints, the higher l/d (i.e. for continuous beams or frames, coefficient k_b is lower than for simply supported beams); 4) the higher the values of creep coefficient and shrinkage strain, the higher is k_t, and the lower is l/d 5) the higher the concrete compressive strength, the higher l/d since, even though n and, consequently k_r, is lower, E_c is higher and k_t is lower.

For a member with given dimensions, materials and reinforcement ratio (i.e. designed to resist at least the design loads at ULS of flexure), Eq. (15) may be used to check whether it is necessary or not to calculate deflections for the verification of its corresponding limit state. Alternatively, Eq. (15) can be used to obtain the reinforcement amount necessary to satisfy the deformation limit state, solving it for k_r, which is directly related to $n\rho$ (see Eq. 9).

2.4. Slenderness associated simultaneously to deflection and reinforcement stress limitations

In order to satisfy the serviceability limit state of cracking, the crack width needs to be limited. The crack width depends on many factors associated to concrete, steel and bond properties, the acting bending moment, the reinforcement ratio and the bars diameter, among others. In particular, the reinforcement stress is a major factor influencing the crack width, so the computation of the average crack width can be avoided if certain relations between the reinforcement stress and the diameter or the spacing of the bars are satisfied, as stated by Eurocode 2 [1] (section 7.3.3 "Control of cracking without direct calculation") and MC2010 (section 7.6.4.6) [2]. For this reason, in this paper, slenderness associated to a maximum allowable reinforcement stress under the quasi-permanent load combination, $\sigma_{s,max}$, will be derived, as a way of limiting the crack width.

The stress in the tension reinforcement, σ_s, in a fully cracked section of rectangular shape or T-shape (when the neutral axis depth is less than the flange depth, $x < h_f$), subjected to a bending moment M_{qp} produced by the quasi-permanent load combination, can be formulated as:

$$\sigma_s = \frac{M_{qp}}{zA_s} \cong \frac{k_g M}{0.9 d\, A_s} = \frac{k_g k_m p l^2}{0.9 \rho b d^2} \leq \sigma_{s,\max} \tag{16}$$

where σ_{smax} is the limiting reinforcement stress to avoid excessive crack width; k_m is a factor relating the support conditions corresponding to the characteristic bending moment, M, with the characteristic load p ($M = k_m \cdot p \cdot l^2$). The lever arm $z = 0.9d$ has been adopted considering a neutral axis depth $x = 0.3d$, which corresponds to an average reinforcement ratio $\rho = 1.0$ %., so that $z = d - x/3 \cong 0.9d$

Solving Eq. (16) for l/d and substituting it into Eq. (15) a slenderness associated to deflections and reinforcement stress limits is obtained:

$$\frac{l}{d} \leq \frac{E_c k_m k_r}{0.9 C \rho \sigma_{s,\max} k_b k_t} \tag{17}$$

Figures 4a and 4b show the slenderness l/d associated to deflection, Eq (15), and reinforcement stress limits, Eq. (17), for different steel reinforcement ratios (ρ) and surface loads (p/b), for simply

supported beams (k_b = 5/384) and for internal spans of continuous beams (k_b = 1/185), respectively, adopting f_{ck} = 30 N/mm^2, φ = 2.5, ε_{cs} = 0.0003, as concrete properties, deflection limitation C = 250 and a ratio of quasi-permanent to total loads k_g = 0.7.

Figure 4a

Figure 4b

A particular case of interest is that associated to the amount of reinforcement strictly necessary for flexural strength (which is the basis for the adjustment of EC2 [1] and MC2010 [2] slenderness limits). In this case, the stress in the reinforcement, under the quasi-permanent load combination, may be estimated as:

$$\sigma_{s,qp} = \frac{k_g f_{yd}}{\gamma_f} \tag{18}$$

where γ_f is the average loads factor, which can be adopted as 1.4 for usual ratios of permanent to live load. The slenderness limit associated to such stress in the reinforcement is, then:

$$\frac{l}{d} \leq \frac{E_c \gamma_f k_m k_r}{0.9 C \rho f_{yd} k_b k_t} \tag{19}$$

which is plotted in Figures 4.a and 4.b as “Strict” stress.

Figure 4b, plotted for an internal span of a continuous beam, has been obtained without considering the possible redistribution of bending moments in continuous beams at service, due to cracking, which may affect the stresses and the deflections. For this reason, it is suggested that, in order to use the above slenderness limits without driving to excessive crack width or to excessively conservative values, limitations on the level of redistributions should be adopted in continuous members. The level of such limitations would require specific studies.

3. VERIFICATION OF THE PROPOSED EQUATIONS WITH A NON-LINEAR TIME-DEPENDENT STRUCTURAL ANALYSIS

3.1. Description of the followed procedure

In order to verify the accuracy of Eqs. (15) and (17) proposed for slenderness limits, two structures have been studied by means of a non-linear time-dependent analysis developed by Marí [31]. The two analyzed structures are a simply supported and a continuous slab of three equal spans. The differences between them are, in addition to those related to boundary conditions, span length and reinforcement ratios. Because the slab is continuous, cracking and delayed deformations may produce time-dependent forces redistributions, thus affecting the deflections. In addition, different environmental relative humidities are considered in each case.

While Eqs. (15) and (17) provide the slenderness ratios associated to limitations in the maximum deflection and stress in the reinforcement, the non-linear analysis is a verification procedure that provides the structural response (in terms of deflections, strains, stresses, internal forces, reactions, etc.) for given dimensions, materials, reinforcement, loads and support conditions. Therefore, the comparison of results is not straightforward, unless the structure analyzed provides exactly a deflection equal to the maximum allowed deflection ($a_{lim} = l/250$, $C = 250$). For this reason, a trial and error procedure has been implemented as follows:

1) Given the geometry (b, h, d, L), boundary conditions of the structure, and the applied loads (g, q, ψ_2), an approximate reinforcement ratio is computed for the ultimate limit state of flexure.
2) A non-linear time-dependent analysis is performed, by first applying the total load ($p = g + q$), and subsequently removing the fraction ($1-\psi_2$) q, to keep the quasi-permanent load until the end of the period of time studied.
3) If the computed maximum deflection, a_{max}, is higher than the limit deflection for quasi-permanent loads ($a_{lim} = l/250$), the reinforcement amount is increased and vice-versa.
4) Steps 2 and 3 are repeated until the maximum deflection is sufficiently close to $l/250$.
5) Once the reinforcement ratio is known, the deformation slenderness ratio is calculated by Eq. (15) and compared with that from the numerical analysis.
6) The reinforcement stress associated to the above obtained slenderness ratio is calculated with Eq. (16) and compared with the stress obtained from the numerical analysis.

3.2. Brief description of the nonlinear and time-dependent analysis model used

The model, implemented in a computer program developed by Marí [32], called CONS, is based on the displacement formulation of the Finite Element Method (FEM), using a beam element with the cross section divided into fibers or filaments subjected to a uniaxial stress state (Figure 5). It is assumed that plane sections remain plane and the deformations due to shear strains are neglected. The materials nonlinearities due to cracking and yielding, and the structural effects of the delayed deformations are taken into account in the structural analysis under loads and imposed deformations.

The total strain at a given time and point in the structure $\varepsilon(t)$, is taken as the direct sum of mechanical strain $\varepsilon^{m}(t)$, and non-mechanical strain $\varepsilon^{nm}(t)$, consisting of creep strain $\varepsilon_{cr}(t)$, shrinkage strain $\varepsilon_{cs}(t)$, aging strain $\varepsilon_{a}(t)$, and thermal strain $\varepsilon_{T}(t)$.

$$\varepsilon\left(t\right)=\varepsilon^{m}\left(t\right)+\varepsilon^{nm}\left(t\right) \tag{20}$$

$$\varepsilon^{nm}\left(t\right)=\varepsilon_{cr}\left(t\right)+\varepsilon_{cs}\left(t\right)+\varepsilon_{a}\left(t\right)+\varepsilon_{T}\left(t\right) \tag{21}$$

Figure 5

The instantaneous nonlinear behavior of concrete in compression has been considered by means of a parabolic model with a post-peak descending branch and load reversal (Figure 6). A smeared crack approach is used and tension stiffening is considered in the tensile stress-strain branch of concrete, adopting for the softening branch the model proposed by Carreira and Chu [33], with a softening parameter $\beta = 3$. Such softening branch could be well approached by a linear descending branch with a slope $m = -0.25\ E_c$. The evolution of concrete mechanical properties due to aging with time have been considered according to the EC2 [1]. For reinforcing steel, a bilinear stress-strain relationship is assumed with load reversals (Figure 7).

Figure 6

Figure 7

Creep strain $\varepsilon_{cr}(t)$ of concrete is evaluated by an age dependent integral formulation based on the principle of superposition. Thus,

$$\varepsilon_{cr}(t) = \int_0^t c(\tau, t-\tau) \frac{\partial \sigma(\tau)}{\partial \tau} d\tau \tag{22}$$

where $c(t, t-\tau)$ is the specific creep function, dependent on the age at loading τ, and $\sigma(\tau)$ is the stress applied at instant τ. Numerical creep analysis may be performed by subdividing the total time interval of interest into time intervals Δt, separated by time steps. The integral (22) can then be approximated by a finite sum involving incremental stress change over the time steps. The adopted form for the specific creep function $c(t, t-\tau)$ is a Dirichlet series:

$$c(\tau, t-\tau) = \sum_{i=1}^{m} a_i(\tau) \left[1 - e^{-\lambda_i (t-\tau)} \right] \tag{23}$$

where m, λ_i, and $a_i(t)$ are coefficients to be determined through adjustment of experimental or empirical creep formulae, as recommended by international codes, by least squares fit. In this work, it is considered that sufficient accuracy is obtained using three terms of the series (m = 3), and adopting λ_i = 10-i. The creep and shrinkage models used are those provided by the MC2010 [2].

The use of a Dirichlet series allows obtaining the creep strain increment at a given instant by a recurrent expression that only requires to store the stress and an internal variable of the last time step, thus avoiding the need to store the entire stress history.

The structural analysis strategy consists of a time step-by-step procedure, in which the time domain is divided into a discrete number of time intervals. A time step forward integration is performed in which increments of displacements, strains and other structural quantities are successively added to the previous totals as we march forward in the time domain. At each time step, the structure is analyzed under the external applied loads and under the imposed deformations, such as creep, originated during the previous time interval and geometry.

Iterative procedures such as Newton-Raphson and Modified Newton or displacement control, combined with incremental analyses are used to trace the structural response along the structure service life throughout the elastic, cracked and ultimate load levels.

Nodal displacements, element internal forces, stresses and strains in each concrete and steel filament, curvature and elongation of each section, support reactions and other response parameters are provided by the model, after convergence is reached. The described model was experimentally checked by Marí and Valdés [34], and has been widely used for the non-linear time-dependent analysis of bridges decks, slender columns and cracked sections by Marí and Hellesland [35].

3.3. Case study 1: Simply supported one-way solid slab.

A simply supported one-way RC solid slab of 6m span and total height of 300 mm (Figure 8) is subjected to a characteristic uniformly distributed load value p = 20 kN/m^2, of which g = 12 kN/m^2 is permanent and q = 8 kN/m^2 corresponds to live load. The quasi-permanent load combination factor is ψ_2 = 0.2 and it is assumed that all loads are applied at 28 days. The slab is reinforced with 5 steel ribbed bars of 20 mm diameter per 1 m width (1570.8 mm^2/m), and the effective depth is 250 mm. Concrete characteristic compressive strength at 28 days is f_{ck} = 30 N/mm^2 (f_{cm} = 38 N/mm^2, E_c = 32836 N/mm^2, f_{ctm} = 2.89 N/mm^2). The environmental relative humidity is RH = 75%, the concrete creep coefficient is φ (28,∞) = 1.8, and the shrinkage strain is ε_{cs} = 0.0003. The reinforcing steel yield strength is f_{yk} = 500 N/mm^2 and the modulus of elasticity is E_s = 200000 N/mm^2.

Figure 8

For the non-linear analysis, 20 equal 1D finite elements of 300 mm length, width b = 1.0 m and total height h = 300 mm, have been used. The cross-section is vertically divided into 30 horizontal layers, each 10 mm thick. At 28 days, the total load p = 20 kN/m is applied, in order to produce a cracking level corresponding to the characteristic load, and subsequently, 80% of the live load (6.4 kN/m) is removed, so that the quasi-permanent load $p + \psi_2 q$ = 12+0.2·8 = 13.6 kN/m is maintained

for 10000 days. A step-by-step non-linear time-dependent analysis is performed using 21 time steps spaced by intervals of increasing length, according to a geometric series. Results of the analysis in terms of deflection, reinforcement and concrete strains and reinforcement stresses are shown in Figures 9, 10 and 11, respectively.

Figure 9

It can be observed that the long-term deflection at mid-span under the quasi-permanent load is 24.1 mm, which is very close to a typical deflection limit given $a_{max} = l/C = l/250 = 24$ mm (being $C = 250$, see Eq. (2). Therefore, it can be considered that the slab slenderness ($l/d = 6000/250 = 24$) is the deflection limit slenderness.

Figure 10 shows the strains in the reinforcement and at the most compressed concrete fiber along time under the quasi-permanent load.

Figure 10

It can be observed that, while the absolute value of the concrete compressive strains increase from ε_c = -0.00048 to ε_c = -0.00092 due to creep and shrinkage, tensile reinforcement strains remain almost constant (with only an increment of 5% approximately). Such results confirm the adequacy of the hypothesis adopted to evaluate the time-dependent curvatures (see Figure 3).

Figure 11 shows the stress in the reinforcement at the midspan section, which varies from 153 to 162 N/mm^2 over time.

Figure 11

The proposed formulation, applied for simply supported members ($l_a = l_c = 0$, $l_b = l$), provides the following results in terms of slenderness limits and stress in the reinforcement:

$$\frac{l}{d} \le \sqrt[3]{\frac{E_c k_r}{C k_b k_g k_t \frac{p}{b}}} = \sqrt[3]{\frac{32836568 \cdot 0.02972}{250 \cdot 0.01301 \cdot 0.68 \cdot 1.73 \cdot 20}} = 23.34$$

where:

$$k_t = 1 + 0.24\varphi + 1000\varepsilon_{cs} = 1 + 0.24 \cdot 1.8 + 1000 \cdot 0.0003 = 1.732$$

$$k_b = \frac{5}{384} = 0.013$$

$$k_g = \frac{g + \psi_2 q}{g + q} = \frac{12 + 0.2 \cdot 8}{12 + 8} = 0.68$$

$$\frac{p}{b} = 20\, kN/m^2$$

$$k_r = 0.0125\left(1 + 36 n \rho\right) = 0.0125\left(1 + 36 \cdot 6.09 \cdot 0.00628\right) = 0.02972$$

It can be observed that the deformation slenderness limit provided by the proposed formulation is very close to that of the slab analyzed (l/d = 23.34 vs l/d = 24, 2.75% error), associated to a_{max} = l/250.

The stress at the reinforcement can be extracted from Eq. (16), as follows:

$$\sigma_s \cong \frac{k_g k_m p l^2}{0.9 \rho b d^2} = \frac{0.68 \cdot 0.125 \cdot 20 \cdot 6^2}{0.9 \cdot 0.00628 \cdot 1 \cdot 0.25^2} 10^{-3} = 173.2\, N/mm^2$$

Such stress, that already includes the tension stiffening effect through factor k_r, is 7% higher than that given by the numerical model (σ_s = 162 N/mm^2).

3.4. Case study 2: Continuous one-way ribbed slab.

Consider a continuous one-way reinforced concrete ribbed slab of three equal spans of 7.5 m length each, subjected to a characteristic uniformly distributed surface load of 15 kN/m^2, of which g = 10 kN/m^2 are permanent and q = 5 kN/m^2 corresponds to live load. The quasi-permanent load combination factor is ψ_2 = 0.2 and it is assumed that all loads are applied at 28 days. The ribbed slab is composed by a top slab of 100 mm depth and rectangular ribs of b = 200 mm and h = 250 mm, spaced 800 mm between ribs axes. Figure 12 shows the longitudinal and cross section

geometry and the reinforcement layout. The total and effective depth of the slab are 300 mm and 250 mm, respectively, and the member slenderness is λ=7.5/0.30=25.

Concrete characteristic compressive strength at 28 days is f_{ck} = 25 N/mm^2 (f_{cm} = 33 N/mm^2, E_c = 31477 N/mm^2, f_{ctm} = 2.56 N/mm^2). The environmental relative humidity is RH = 60%, the concrete creep coefficient is φ = 2.6, and the shrinkage strain is ε_{cs} = 0.0005. The reinforcing steel yield strength is f_{yk} = 500 N/mm^2 and the modulus of elasticity is E_s = 200000 N/mm^2. The maximum deflection (which takes place at the exterior spans) should be less than l/250 = 30 mm.

Figure 12

In the following, all calculations will be made for a strip of the slab considering a T-section with a flange width of 800 mm (distance between ribs axes). The uncracked inertia of the section is I_b = 0.001276 m^4, the centre of gravity is at a distance v = 0.117 m from the top, and the cracking moment under positive and negative flexure (tensile stresses at bottom and top, respectively) are $M_{cr,p}$ = 14 kNm and $M_{cr,n}$ = 27.9 kNm.

For the non-linear analysis, 60 equal 1D finite elements of 375 mm length, have been used. The cross-section is divided into 35 horizontal layers, each 10 mm thick. At 28 days, the characteristic load per unit length p = 15 kN/m^2·0.8 m = 12 kN/m is applied, in order to produce a cracking level corresponding to the characteristic load combination, and subsequently, 80% of the live load (q = 5 kN/m^2·0.8 m = 4 kN/m) is removed, so that the quasi-permanent load $p + \psi_2 q$ = 8 + 0.2·4 = 8.8 kN/m is maintained for 10000 days. The deflections and stresses obtained by means of the nonlinear analysis are shown in Figures 13 and 14, respectively.

Figure 13

It can be seen that the long-term deflection due to quasi-permanent load combination is almost exactly 30 mm, which corresponds to a fraction of the length l/250, which is the target deflection.

Figure 14

The proposed formulation provides the following results in terms of slenderness limits and stress in the reinforcements.

$$\frac{l}{d} \le \sqrt[3]{\frac{E_c k_r}{C k_b k_g k_t \frac{p}{b}}} = \sqrt[3]{\frac{31476000 \cdot 0.0205}{250 \cdot 0.00668 \cdot 0.733 1.969 \cdot \frac{12}{0.8}}} = 26.13$$

The following values of the design parameters have been used:

$$\rho_a = 0; \qquad \rho_b = \frac{930}{200 \cdot 300} = 0.0155; \quad \rho_c = \frac{804}{800 \cdot 300} = 0.00335;$$

$$k_{rs,a} = 0$$

$$k_{rs,b} = 0.0125\left(1 + 36 n \rho_b\right) = 0.0568$$

$$k_{rs,c} = 0.0125\left(1 + 36 n \rho_c\right) = 0.0221$$

$$k_r = k_{rs,a} \frac{l_a}{l} \frac{b_a}{b_c} + k_{rs,b} \frac{l_b}{l} \frac{b_b}{b_c} + k_{rs,c} \frac{l_c}{l} = 0.0568 \cdot 0.2 \cdot \frac{200}{800} + 0.0221 \cdot 0.8 = 0.0205$$

$$\rho'_a = 0; \quad \rho'_b = \frac{402}{200 \cdot 300} = 0.0067; \quad \rho'_c = \frac{302}{800 \cdot 300} = 0.001257$$

$$k_{t,b} = 1 + \frac{0.24\varphi + 1000\varepsilon_{cs}}{1 + 12 n \rho'_b} = 1 + \frac{0.24 \cdot 2.6 + 1000 \cdot 0.0005}{1 + 12 \cdot 6.35 \cdot 0.0067} = 1.744$$

$$k_{t,c} = 1 + \frac{0.24\varphi + 1000\varepsilon_{cs}}{1 + 12 n \rho'_c} = 1 + \frac{0.24 \cdot 2.6 + 1000 \cdot 0.0005}{1 + 12 \cdot 6.35 \cdot 0.001257} = 2.026$$

$$k_t = k_{t,a} \frac{l_a}{l} + k_{t,b} \frac{l_b}{l} + k_{t,c} \frac{l_c}{l} = 1.744 \cdot 0.2 + 2.026 \cdot 0.8 = 1.969$$

$$k_b = \frac{5}{384} - \frac{0.1}{9\sqrt{3}} = 0.00668$$

$$k_g = \frac{g + \psi_2 q}{g + q} = \frac{8 + 0.2 \cdot 4}{8 + 4} = 0.733$$

$$\frac{p}{b} = \frac{12}{0.8} = 15 kN/m^2$$

The factor k_b used is that corresponding to the external span, where the negative moment over the interior support is $M = 0.1\ pl^2$, obtained elastically, (i.e. without accounting for moments redistribution due to cracking).

It can be observed that the deformation slenderness limit provided by the proposed formulation is (l/d = 26.13 which is 4.5% higher than the slab slenderness, l/d = 25, associated to $a_{max} = l/250$. Probably this difference is due to not considering the effects of moment redistribution in the deflections.

The stress at the tensile reinforcement at center span, according to Eq (16) is:

$$\sigma_s \simeq \frac{k_g k_m p l^2}{0.9 \rho b d^2} = \frac{0.733 \cdot 0.08 \cdot 12 \cdot 7.5^2}{0.9 \cdot 0.00335 \cdot 0.8 \cdot 0.3^2} = 182.3\, N/mm^2$$

That value is only 5.8% higher than that obtained by the numerical model for long term (σ_s = 172 N/mm^2).

As a conclusion it can be said that even the complexity of the instantaneous and long-term structural response due to cracking, creep, shrinkage, etc., the proposed equations for slenderness limits provide quite good results, when compared with the results of a non-linear time dependent finite element analysis. Therefore, the derived slenderness limits can be very useful for design purposes.

4. COMPARISON OF THE PROPOSED SLENDER LIMITS WITH THE RESULTS OBTAINED BY USING THE EUROCODE EC2 PROPOSAL FOR CALCULATION OF DEFLECTIONS

To further analyze the capacity of the proposed method to obtain reasonable values of the slenderness limit, a comparison with results obtained using the EC2 [1], for the computation of deflections, is made in this section. According to previous sections, the analysis has been done for values of l/d obtained for constant load, as well as for constant stress. The calculations have been performed as indicated in the following text.

For the case of constant load, given a specific reinforcement ratio and sectional characteristics, a span length, l, is assumed, allowing to obtain long-term deflections due to quasi-permanent load from an effective moment of inertia calculated on the basis of interpolation between uncracked and fully cracked sections [1-2]. The level of cracking for obtaining the effective moment of inertia is calculated by using the characteristic load. Trying different values of the span length, the slenderness is obtained dividing l by d, when the deflection is $l/250$.

A similar procedure has been used for the case of constant stress due to quasi-permanent loads. For a given reinforcement ratio, and a value of the stress in the tensile reinforcement, the service flexural moment for the critical section can be obtained. Again values for l are tried and the slenderness limit is obtained when the deflection is $l/250$.

This global procedure is not different from that used in other works [21, 24, 36] for obtaining the l/d value corresponding to the maximum bending moment associated to a given reinforcement ratio (strict value). However, here the values are obtained also for lower loads than those corresponding to the flexural capacity of the section, which is usually the case in practice.

Figure 15 shows the comparison for values of p/b of 10, 25, 50 and 100 kN/m^2, for assumed parameters f_{yk} = 500 N/mm^2, k_g = 0.7, ratio of permanent-to-total load = 0.6, γ_f = 1.41, and for f_{ck} = 30 N/mm^2 (φ = 2.5, $\varepsilon_{cs} = 500 \cdot 10^{-6}$) and f_{ck}=50 N/mm^2 (φ = 1.5, $\varepsilon_{cs} = 400 \cdot 10^{-6}$). Figures 15a and 15b show similar values for the slenderness limits under constant load, although an influence of the concrete strength around 10% is observed (higher strength concrete allows slenderer beams). Only those cases with reinforcement stress, due to quasi-permanent loads, higher than 70 N/mm^2 have been represented in Figures 15a and b, to avoid non-realistic situations. An increase of l/d is seen for an increase of reinforcement ratio with constant load. A logical reduction in l/d is showed for increasing loads.

The proposed method (PM in Figures 15a and 15b) follows reasonably well the values obtained with a much more complex model, such as that from EC2 [1]. Statistical values (average, maximum, minimum and coefficient of variation) of the ratio between slenderness limits obtained with the proposed method and that from EC2 [1] are shown in Table 1. It is seen that average

589 values are quite close to the unity. Maximum differences are obtained for the lowest load level, and
590 as the load increases the curves are practically identical.
591
592 Figure 15
593 Table 1
594
595 Figure 16 shows the comparison for values of constant stress of 150 N/mm^2 due to quasi-
596 permanent loads, as well as those obtained for the maximum permissible stress under serviceability
597 conditions, corresponding to that of the steel yielding strength for ultimate limit state ($f_{yd} = f_{yk}/\gamma_s$ =
598 500/1.15 = 435 N/mm^2), which is named in the figures as "σ strict". As indicated previously, in
599 these circumstances the quasi-permanent stress would be $f_{yd} \cdot k_g/\gamma_f$ = 435·0.7/1.41 = 216 N/mm^2. For
600 comparison purposes another curve called "EC2-A_s strict" is also presented. This curve is obtained
601 using the procedure that was followed for obtaining the EC2 [1] slenderness ratios. It represents the
602 values corresponding to the service moment obtained from the ultimate bending moment
603 corresponding to a given reinforcement ratio. The difference with the "σ strict" curve is that in this
604 case the maximum bending moment is calculated under ULS, while in the previous case is
605 calculated from serviceability conditions (limiting the quasi-permanent service stress); the
606 difference in the lever arms in the calculation gives the slightly different curves.
607
608 Figure 16
609 Table 2
610
611 Figures 16a and 16b, for f_{ck} = 30 N/mm^2 and f_{ck} = 50 N/mm^2, respectively show similar trends,
612 although a relevant influence of the concrete strength on the slenderness value is again observed
613 (around 25% larger for the higher strength for intermediate values of reinforcement ratio). As seen
614 in subsection 2.4 an increase in reinforcement ratio causes a reduction in *l/d*, since keeping the
615 stress constant leads to a higher flexural moment to be sustained. Statistical values of the ratios

between both methods are reported in Table 2, showing that the proposed method provides acceptable values for design.

Furthermore, the assumption made about constant strain in the tensile reinforcement along the time may deviate from the actual value for low reinforcement ratios. In any case, the errors are of acceptable magnitude and on the safe side.

5. CONCLUSIONS

The following conclusions can be drawn from the previous discussion:

- Slenderness limits (l/d) for RC beams, associated to given limitations of deflections under the quasi-permanent load combination and limitations of stresses in the reinforcing steel, for crack control, have been derived. Reinforcement ratio, loading level, materials properties and support conditions are accounted for in the derived expressions, which are simple and, therefore, useful for design, either to know the minimum beam depth or the minimum reinforcement ratio necessary to avoid calculation of deflections or excessive crack width.
- A very simple expression has been derived for k_r, which multiplied by bd^3 provides a very good approach to the effective moment of inertia of a cracked beam, to be used for the calculation of instantaneous deflections according to the bilinear method adopted by EC2 [1]. This factor takes into account "tension stiffening" effects, depends linearly on the homogenized tensile reinforcement ratio $n\rho$ and is independent of the tensile stress.
- Another very simple and useful expression has been derived, see Annex 1, for a time-dependent deflections factor, k_t, which allows obtaining the long-term curvature due to concrete creep and shrinkage, from the instantaneous curvature due to quasi-permanent loads. This factor explicitly depends on the concrete creep coefficient and shrinkage strain and on the compression reinforcement ratio.
- The formulation is valid for simply supported beams, cantilevers and continuous beams. In the latter case, mean global member factors k_r and k_t have been derived to account for the effects of the tensile and compressive reinforcement ratios and effective inertia

distributions along the member length, so that beams with T shaped section can be also covered.

- The results obtained by applying the proposed slenderness limits have been compared with those provided by a non-linear and time-dependent analysis of two case studies: one consisting of a simply supported solid slab and another consisting of a three span continuous ribbed slab. Excellent results have been obtained in such comparisons, despite the complexity of the observed non-linear and time dependent behavior of cracked concrete structures.
- A comparative study has been made between the proposed slenderness limits and those obtained by calculating the long-term deflections by means of Eurocode 2 [1]. The influence of reinforcement ratio, concrete strength, levels of load and stress have been studied. Very good agreement has been obtained for the most common cases, although differences up to 17 % (on the side of safety) have been found.
- The way in which the slenderness limits have been obtained, based on the mechanics of reinforced concrete and on an experimentally verified hypothesis about the time-dependent behavior of cracked sections, allows its application to a large variety of structural situations (i.e. support constraints, environmental conditions, materials properties, quasi-permanent load factors, etc). Furthermore, the mechanical character of the formulation facilitates its modification to other situations different to those used for its derivation, for example different load types, partially pre-stressed or post-tensioned beams use of FRP reinforcement and even moderately axially loaded columns under lateral forces, among others.

Acknowledgements

The authors want to acknowledge the financial support provided by the Spanish Ministry of Economy and Competitiveness (MINECO) and the European Funds for Regional Development (FEDER), through the Research projects: BIA2015-64672-C4-1-R and BIA2017-84975-C2-2-P.

In addition, the authors want to acknowledge the support provided by the Spanish Ministry of Economy and Competitiveness (MINECO) through the Excellence network BIA2017-90856-REDT.

REFERENCES

[1] CEN Eurocode 2: Design of concrete structures. Part 1-1: General rules and rules for buildings. En1992-1-1, Euro. Comm. Stand., Brussels, 2004.

[2] Fédération International du Béton (fib). Model Code for Concrete Structures 2010. Verlag Ernst & Sohn, Berlin; 2013.

[3] ACI-Committee-318 American Concrete Institute. ACI318-11. Building Code Requirements of Structural Concrete and Commentary. 2011. ACI; 2011.

[4] Comité Euro-International du Béton. Cracking and deformations. Design Manual. 1983.

[5] Gilbert, RI. Deflection calculation for reinforced concrete structures-why we sometimes get it wrong. ACI Struct J 1999;96:1027–32.

[6] Bischoff PH, Scanlon A. Effective moment of inertia for calculating deflections of concrete members containing steel reinforcement and fiber-reinforced polymer reinforcement. ACI Struct J 2007;104:68–75.

[7] Marí A, Bairán J, Duarte N. Long-term deflections in cracked reinforced concrete flexural members. Eng Struct 2010;32:29–42.

[8] Gribniak V, Bacinskas D, Kacianauskas R, Kaklauskas G, Torres L. Long-term deflections of reinforced concrete elements: Accuracy analysis of predictions by different methods. Mech Time-Dependent Mater 2013;17:297–313. doi:10.1007/s11043-012-9184-y.

[9] Rangan V. Control of beam deflections by allowable span-depth ratios. ACI J 1982:372–7.

[10] ACI-Committee-318 American Concrete Institute. ACI 318-77. Building Code Requirements for Reinforced Concrete. Detroit, USA: 1977.

[11] Gilbert RI. Deflection control of slabs using allowable span to depth ratios. ACI J 1985:67–72.

[12] Scanlon A, Choi BS. Evaulation of ACI 318 minimum thickness requirements for one-way

699 slabs. ACI Struct J 1999;96:616–21.
700 [13] ACI-Committee-318 American Concrete Institute. ACI 318-95. Building code requirements
701 for structural concrete (ACI 318-95) and commentary (ACI 318R-95). Farmington Hills,
702 Michigan, USA: 1995.
703 [14] Lee YH, Scanlon A. Comparison of one- And two-way slab minimum thickness provisions
704 in building codes and standards. ACI Struct J 2010;107:157–63.
705 [15] ACI-Committee-318. American Concrete Institute. ACI 318-08. Building code
706 requirements for structural concrete (ACI 318-08) and commentary. Farmington Hills,
707 Michigan, USA: 2008.
708 [16] Structural use of concrete, BS8110: Part 1-code of practice for design and construction.
709 London 1997.
710 [17] Standards Australia. Concrete Structures: AS3600-2001. North Sidney, Australia: 2001.
711 [18] Scanlon A, Lee YH. Unified span-to-depth ratio equation for nonprestressed concrete beams
712 and slabs. ACI Struct J 2006;103:142–8. doi:10.14359/15095.
713 [19] Bischoff PH, Scanlon A. Span-depth ratios for one-way members based on ACI 318
714 deflection limits. ACI Struct J 2009;106:617–26.
715 [20] Bischoff PH. Reevaluation of Deflection Prediction for Concrete Beams Reinforced with
716 Steel and Fiber Reinforced Polymer Bars. Struct Eng 2005;131 (5):752–67.
717 [21] Caldentey AP, Cembranos JM, Peiretti HC. Slenderness limits for deflection control: A new
718 formulation for flexural reinforced concrete elements. Struct Concr 2017;18:118–27.
719 doi:10.1002/suco.201600062.
720 [22] Gardner NJ. Span/thickness limits for deflection control. ACI Struct J 2011;108:453–60.
721 [23] Balázs GL, Borosnyói A. Models for Flexural Cracking in Concrete: the State of the Art.
722 Struct Concr 2005;6:53–62. doi:10.1680/stco.2005.6.2.53.
723 [24] Pérez Caldentey A, Corres Peiretti H, Giraldo Soto A, Peset Iribarren J. Cracking of RC
724 members revisited influence of cover, φρs,ef an experimental and theoretical study.pdf.
725 Struct Concr 2013;14:69–78.
726 [25] Gergely P, Lutz LA. Maximum carck width in reinforced concrete flexural members.

Causes, Mech Control Crack Concr SP20 1968;American C:87–117. doi:10.14359/17348.

[26] Frosch RJ. Another look at cracking and crack control in reinforced concrete. ACI Struct J 1999;96:437–42. doi:10.14359/679.

[27] Barris C, Torres L, Miàs C, Vilanova I (2012) "Design of FRP RC beams for serviceability requirements", Journal of Civil Engineering and Management, 18(6): 843-857.

[28] Clarke G, Scholz H, Alexander A. New method to predict the creep deflection of craked reinforced concrete fexural members. ACI Mater J 1988.

[29] Murcia J. Approximate Time Dependent Analysis of Reinforced Concrete Sections. Proposal of a New Factor for the Calculation of Long Term Deflections (in Spanish). Hormigón y Acero 1991;181:9–17.

[30] Bazant ZP. Prediction of Concrete Creep Effects Using Age-Adjusted Effective Modulus Method. J Proc 1972;69:212–9. doi:10.14359/11265.

[31] Marí AR. Numerical simulation of the segmental construction of three dimensional concrete frames. Eng Struct 2000;22:585–96.

[32] Marí AR. Numerical simulation of the segmental construction of three dimensional concrete frames. Eng Struct ELSEVIER 2000;22:585–96.

[33] Carreira, Domingo .J and Chu, Kuang-Han" Stress-Strain Relationship for Reinforced Concrete in Tension", ACI Journal, January-February 1986, pp 21-28

[34] Marí AR, Valdés M. Long-term behavior of continuous precast concrete girder bridge model. J Bridg Eng 2000;5. doi:10.1061/(ASCE)1084-0702(2000)5:1(22).

[35] Mari AR, Hellesland J. Lower slenderness limits for rectangular reinforced concrete columns. J Struct Eng 2005;131:85–95. doi:10.1016/(ASCE)0733-9445(2005)131:1(85).

[36] Corres Peiretti H, Pérez Caldentey A, López Agüí J, Erdtbauer J. PrEN Chapter 7— Serviceability Limit States. Deflections: Supporting Document. The European Concrete Platform ASBL. Brussels: Eurocode 2 Commentary. European Concrete Platform; 2003. doi:doi:10.13140/2.1.4146.0804.

ANNEX 1. SIMPLIFIED SECTIONAL TIME DEPENDENT ANALYSIS

Consider the time dependent deformation of a cracked RC rectangular cross section, as indicated in Figure 3. Due to creep and shrinkage of concrete, a redistribution of forces between concrete and reinforcement takes place. Thus, relaxation of the maximum concrete stress at top fiber and increment in the neutral axis depth takes place along the time. Assuming the simplification of no increment of stress at the tensile reinforcement, the equilibrium of internal forces is expressed by the following equation:

$$\frac{1}{2}\sigma_{c0} b x_0 - \frac{1}{2}\sigma_c b x = A_s^{'}\Delta\sigma_s^{'} = A_s^{'} E_s \Delta\varepsilon_s^{'} \quad \text{(A1.1)}$$

where x_0 is the depth of the concrete stress block at $t = t_0$; x is the depth of the concrete stress block at $t \geq t_0$; σ_{c0} is the maximum concrete stress at $t = t_0$; σ_c is the maximum concrete stress at $t \geq t_0$; A'_s is the compressive steel reinforcement; $\Delta\sigma'_s$ is the increment of stress in the internal compressive steel reinforcements at $t \geq t_0$; E_s is the steel modulus of elasticity; and $\Delta\varepsilon'_s$ is the increment of stress in the internal compressive steel reinforcements at $t \geq t_0$.

Since planar deformation is assumed, compatibility of strains of the deformed section is formulated as follows:

$$\frac{\Delta\varepsilon_s^{'}}{d - d^{'}} = \frac{\Delta\varepsilon_c}{d} \rightarrow \Delta\varepsilon_s^{'} = \Delta\varepsilon_c \frac{d - d^{'}}{d} = \Delta\varepsilon_c \left(1 - \frac{d^{'}}{d}\right) \quad \text{(A1.2)}$$

Substituting $\Delta\varepsilon'_s$ of Eq (A1.2) into Eq. (A1.1), multiplying it by 2/(bx) and after some rearrangements, Eq. (A1.1) becomes:

$$\sigma_c = \sigma_{c0} \frac{x_0}{x} - \frac{2A_s^{'}E_s}{bx}\left(1 - \frac{d^{'}}{d}\right)\Delta\varepsilon_c \quad \text{(A1.3)}$$

Then, the variation of concrete stress results:

$$\Delta\sigma_c = \sigma_c - \sigma_{c0} = \sigma_{c0}\left(\frac{x_0}{x} - 1\right) - \frac{2A_s^{'}E_s}{bx}\left(1 - \frac{d^{'}}{d}\right)\Delta\varepsilon_c \quad \text{(A1.4)}$$

According to the Age Adjusted Effective Modulus Method (AAEMM), the total time dependent concrete strain under variable stress is:

778 $$\Delta\varepsilon_c = \frac{\sigma_{c0}}{E_{c0}}\varphi + \frac{\Delta\sigma_c}{E_{c0}}\left(1+\chi\varphi\right) + \varepsilon_{cs} \quad \text{(A1.5)}$$

779 where $\Delta\sigma_c$ is the variation of concrete stress from t_0 to $t > t_0$; φ is the concrete creep coefficient at

780 time $t \geq t_0$; χ is the concrete aging coefficient at time $t \geq t_0$

781 Substituting Eq. (A1.4) into Eq. (A1.5):

782 $$\Delta\varepsilon_c = \frac{\sigma_{c0}}{E_{c0}}\varphi + \frac{\left(1+\chi\varphi\right)}{E_{c0}}\left[\sigma_{c0}\left(\frac{x_0}{x}-1\right) - \frac{2A_s'E_s}{E_{c0}bx}\left(1-\frac{d'}{d}\right)\Delta\varepsilon_c\right] + \varepsilon_{cs} \quad \text{(A1.6)}$$

783 Then, the time-dependent strain at the top concrete fiber can be expressed as:

784 $$\Delta\varepsilon_c = \frac{\frac{\sigma_{c0}}{E_{c0}}\left[\varphi+\left(\frac{x_0}{x}-1\right)\left(1+\chi\varphi\right)\right]+\varepsilon_{cs}}{1+\frac{2A_s'E_s}{E_{c0}bx}\left(1-\frac{d'}{d}\right)\left(1+\chi\varphi\right)} = \frac{\frac{\sigma_{c0}}{E_{c0}}\left[\varphi+\left(\frac{x_0}{x}-1\right)\left(1+\chi\varphi\right)\right]+\varepsilon_{cs}}{1+\frac{2n\rho'}{\left(\frac{x_0}{d}\right)}\frac{x_0}{x}\left(1-\frac{d'}{d}\right)\left(1+\chi\varphi\right)} \quad \text{(A1.7)}$$

785 where $\rho' = A_s'/bd$ and $n = E_s/E_c$. For practical applications, approximate but conservative values of

786 $\chi = 0.8$, $x_0/x = 0.75$, $d'/d = 0.15$ can be adopted, resulting in:

787 $$\Delta\varepsilon_c = \frac{\frac{\sigma_{c0}}{E_{c0}}\left[\varphi+\left(0.75-1\right)\left(1+0.8\varphi\right)\right]+\varepsilon_{cs}}{1+\frac{2n\rho'}{\left(\frac{x_0}{d}\right)}0.75\left(1-0.15\right)\left(1+0.8\varphi\right)} = \frac{\frac{\sigma_{c0}}{E_{c0}}\left[0.8\varphi-0.25\right]+\varepsilon_{cs}}{1+\frac{1.275n\rho'}{\left(\frac{x_0}{d}\right)}\left(1+0.8\varphi\right)} \leq \frac{\frac{\sigma_{c0}}{E_{c0}}0.8\varphi+\varepsilon_{cs}}{1+12n\rho'} \quad \text{(A1.8)}$$

788 where expression 0.8φ-0.25 has been substituted by 0.8φ, which is conservative, and in the

789 denominator, a instantaneous neutral axis depth $x_0/d = 0.3$ and $\varphi = 2.5$ have been adopted.

790 The time-dependent increment of curvature, $\Delta\psi$, can be expressed as:

791 $$\Delta\psi\left(t\right) = \frac{\Delta\varepsilon_c}{d} = \left(\frac{1}{d}\right)\frac{\frac{\sigma_{c0}}{E_{c0}}0.8\varphi+\varepsilon_{cs}}{1+12n\rho'} = \left(\frac{1}{d}\right)\frac{\varepsilon_{c0}0.8\varphi+\varepsilon_{cs}}{1+12n\rho'} = \frac{\varepsilon_{c0}}{d}\frac{0.8\varphi+\frac{\varepsilon_{cs}}{\varepsilon_{c0}}}{1+12n\rho'} \quad \text{(A1.9)}$$

792 which can be rewritten as:

793 $$\Delta\psi\left(t\right) = \frac{\varepsilon_{c0}}{x_0}\frac{x_0}{d}\frac{0.8\varphi+\frac{\varepsilon_{cs}}{\varepsilon_{c0}}}{1+12n\rho'} = \psi_0\frac{x_0}{d}\left(k_\varphi\varphi + k_{cs}\varepsilon_{cs}\right) \quad \text{(A1.10)}$$

where ε_{c0}, x_0 and $\psi_0 = \varepsilon_{c0}/x_0$ are the instantaneous concrete compressive maximum strain, the neutral axis depth and the instantaneous curvature due to quasi-permanent load combination of the cracked section, respectively.

The creep and shrinkage reduction factors, k_φ and k_{sh}, respectively, take into account the effects of the stresses relaxation and ageing of concrete, as well as the constraint introduced by the compressive reinforcement to the time dependent deformation:

$$k_\varphi = \frac{0.8\varphi}{1+12n\rho'}; \quad k_{cs} = \frac{1}{\varepsilon_{c0}\left(1+12n\rho'\right)}$$

(A1.11)

Then, the time dependent deflection factor k_t, which, assuming the same behavior along the element length can be adopted as time dependent deflection factor in Eq. (2), is:

$$k_t = \frac{\psi(t)}{\psi_0} = \frac{\psi_0 + \Delta\psi(t)}{\psi_0} = 1 + \frac{\Delta\psi(t)}{\psi_0} = 1 + \left(k_\varphi\varphi + k_{cs}\varepsilon_{cs}\right)\frac{x_0}{d} \qquad \text{(A1.12)}$$

Adopting $\varepsilon_{c0} = 0.3\ f_c/E_c$ for the maximum concrete strain produced by the quasi-permanent load, $x_0/d = 0.3$ and $E_c/f_c = 1000$, as average values, which correspond to a reinforcement ratio of 1% and to $f_c = 35$ N/mm^2, the time-dependent deflection factor, k_t, becomes:

$$k_t = 1 + \left(k_\varphi\varphi + k_{cs}\varepsilon_{cs}\right)\frac{x_0}{d} \simeq 1 + \frac{\left(0.8\varphi + \dfrac{E_{c0}\varepsilon_{cs}}{0.3\,f_c}\right)}{1+12n\rho'}\frac{x_0}{d} \simeq 1 + \frac{0.24\varphi + 1000\varepsilon_{cs}}{1+12n\rho'} \qquad \text{(A1.13)}$$

809 List of Figures

810

List of Tables

836

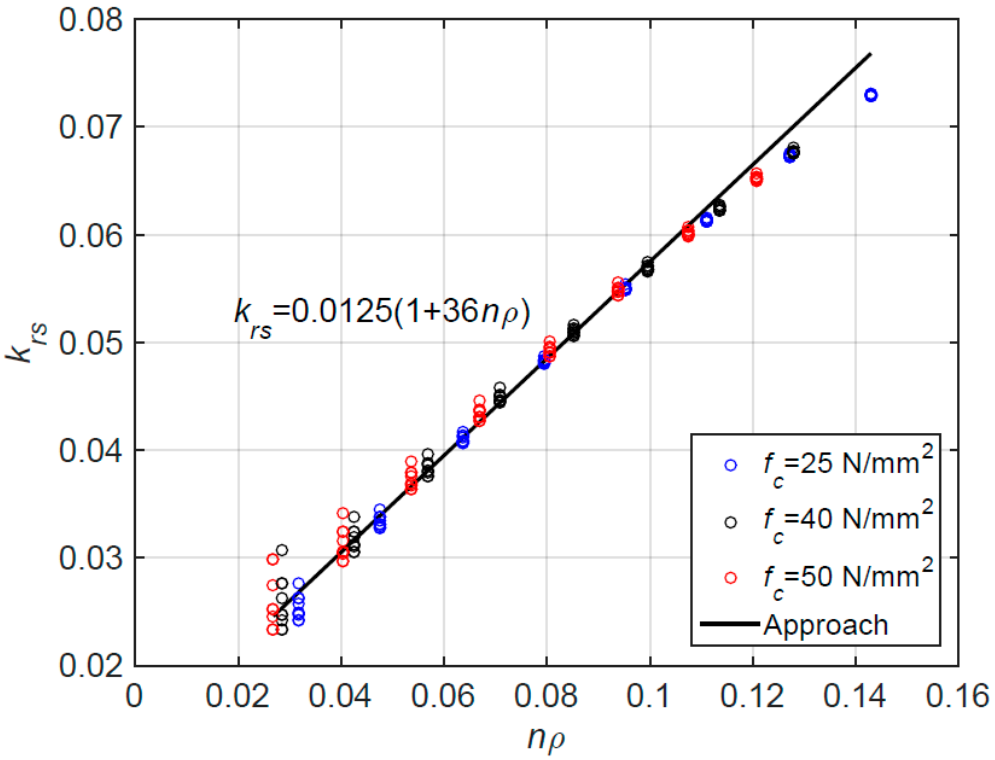

837

838 Figure 1: Simplified dimensionless effective moment of inertia of a cracked section

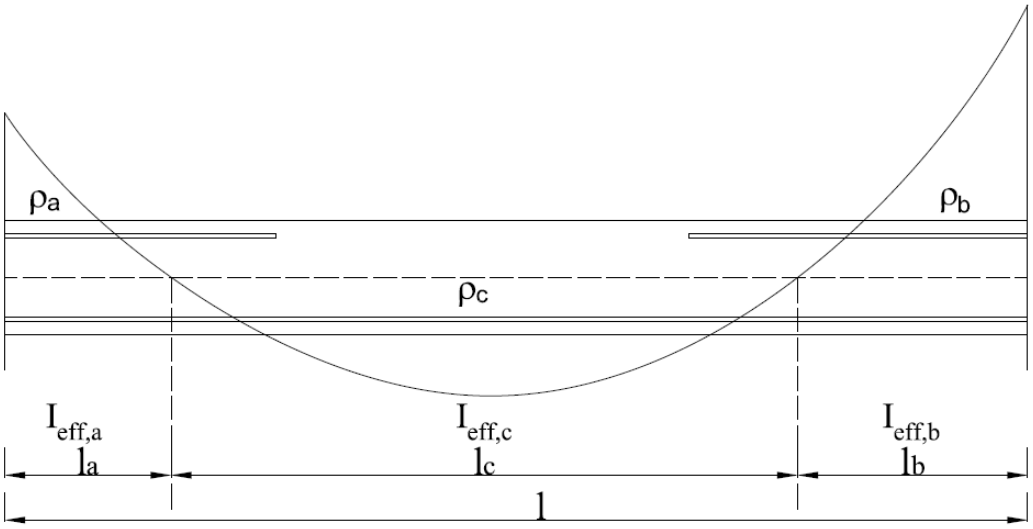

839

840 Figure 2. Definition of lengths l_a, l_b and l_c along a continuous beam

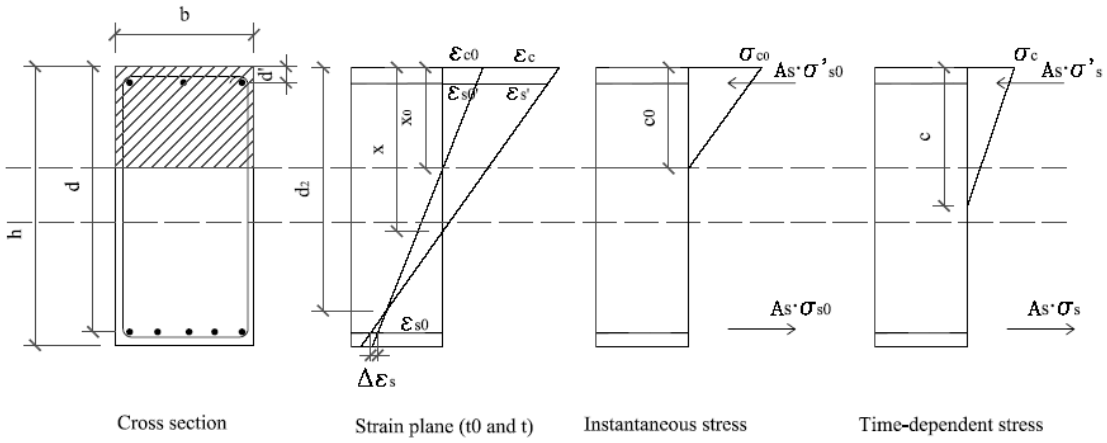

841

842 Figure 3. Time-dependent increment of stresses and strains in a RC cracked section.

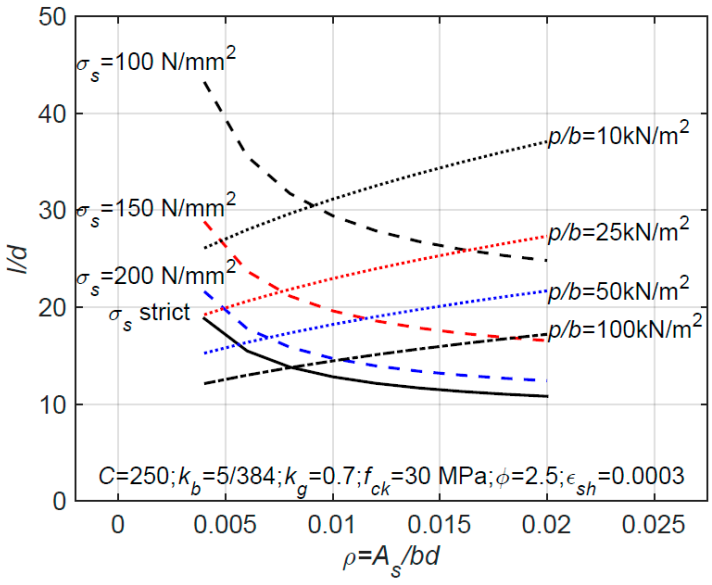

843

844 (a)

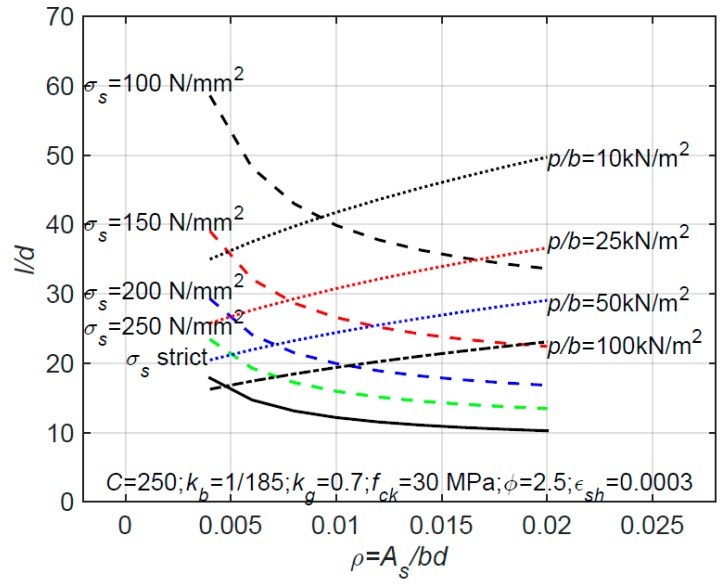

845

846 (b)

847

848 Figure 4. Deformation and stress limitation slenderness ratios, (a) simply supported beams, (b)

849 external span continuous beams.

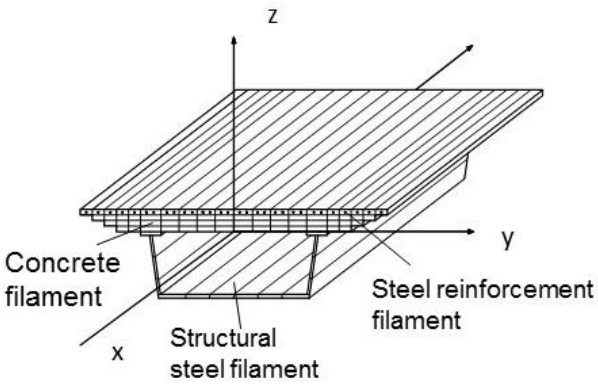

850

851 Figure 5. Filament beam element.

852

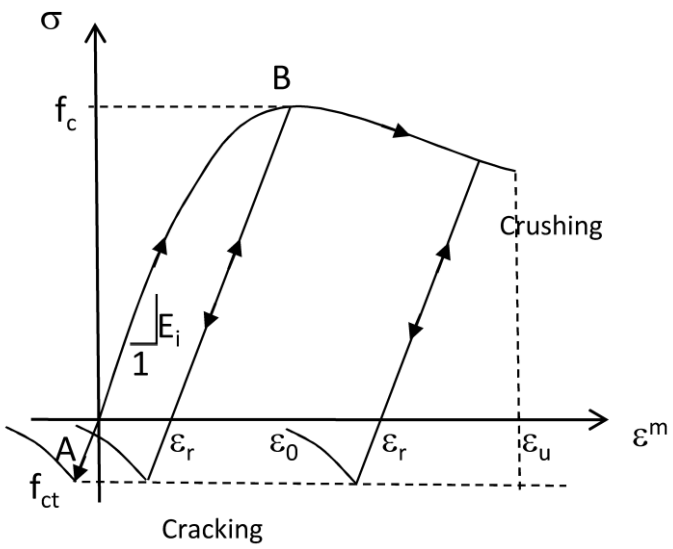

853

854 Figure 6. Concrete instantaneous stress-strain adopted.

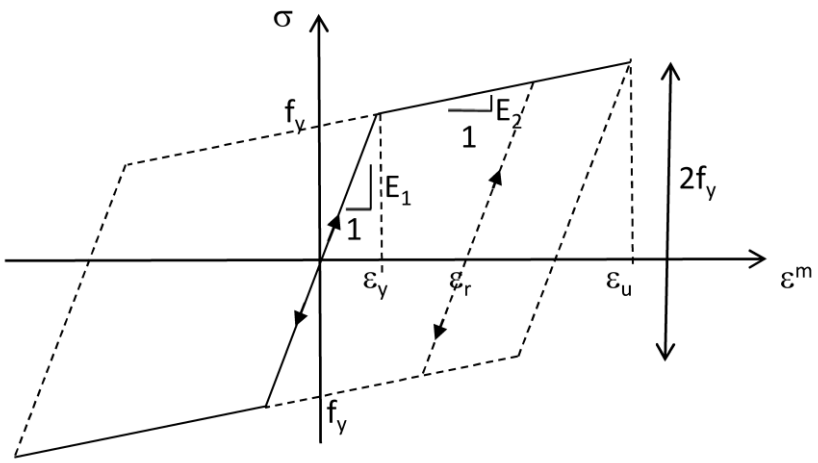

855

856 Figure 7. Reinforcing steel stress-strain.

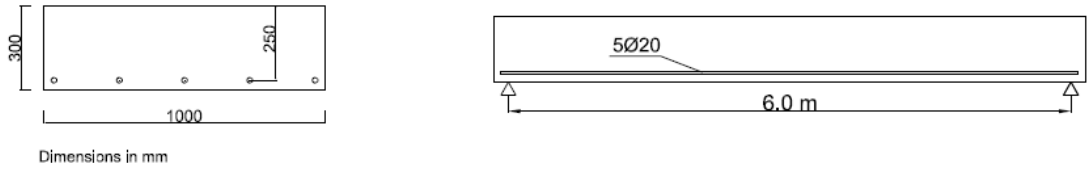

857

858 Figure 8. Simply supported one-way slab analyzed in case study 1.

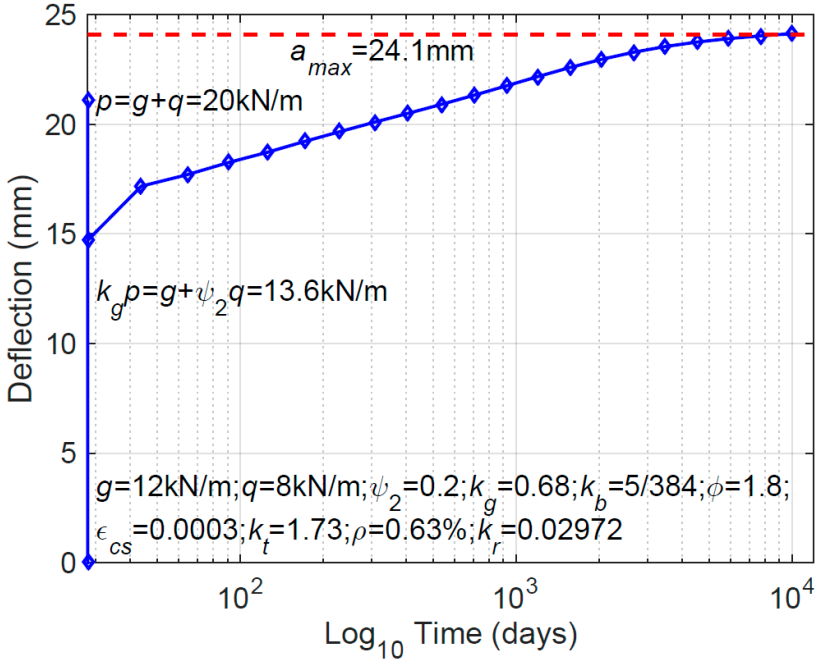

859

860 Figure 9. Displacements at mid-span of the simply supported one-way slab along the time

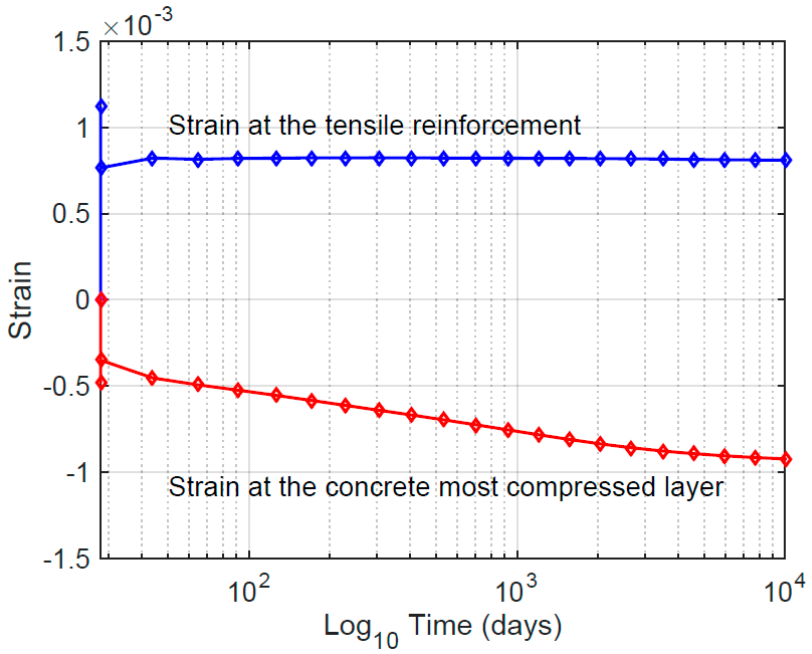

861

862 Figure 10. Strains at the tensile reinforcement at mid-span along the time for case study 1.

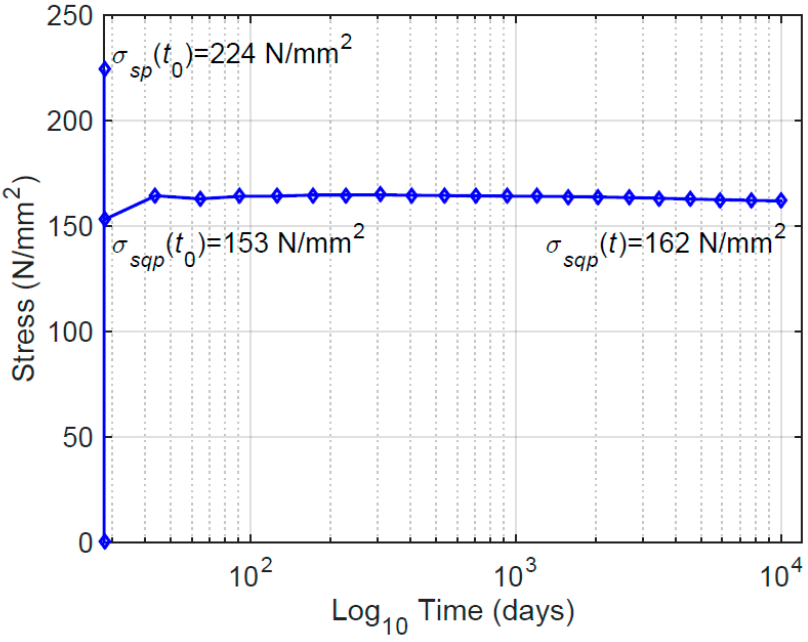

863

864 Figure 11. Stresses at the tensile reinforcement along the time, for case study 1.

865

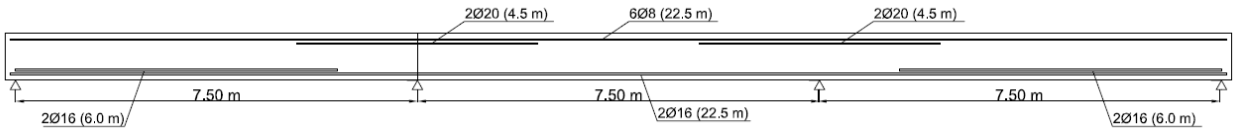

866

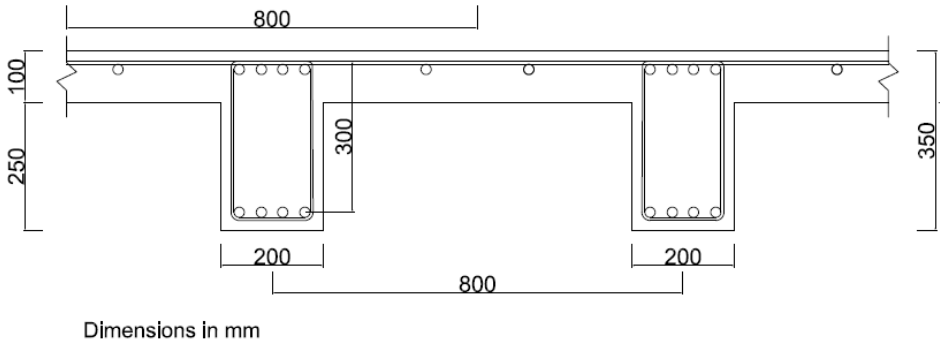

867

868 Figure 12. Continuous ribbed slab analyzed in case study 2.

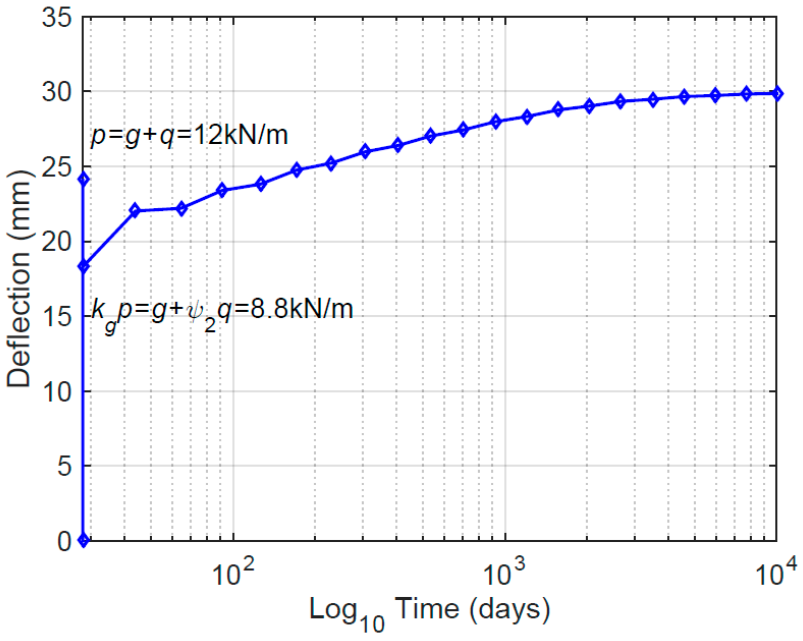

869

870 Figure 13. Deflection at the lateral span, along the time

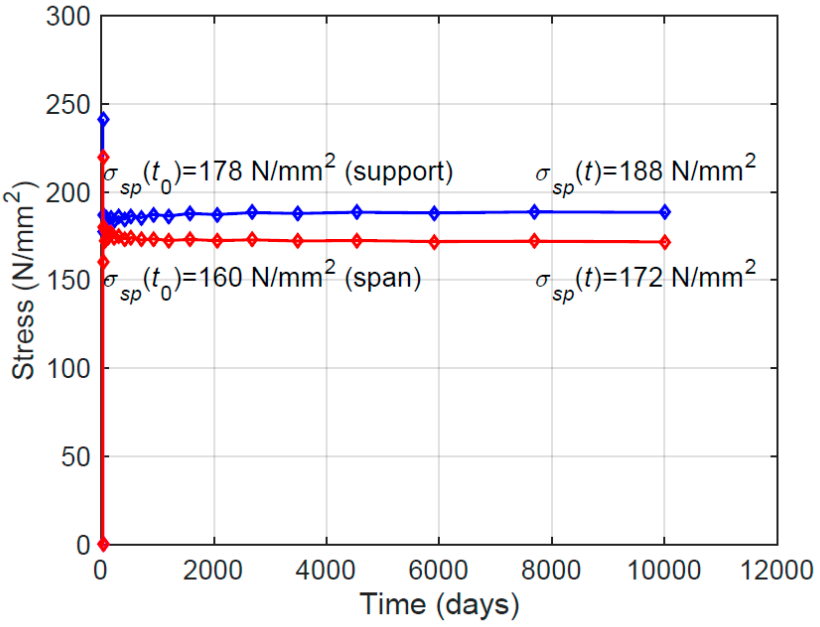

871

872 Figure 14. Stress at the tensile reinforcement at span and over the support

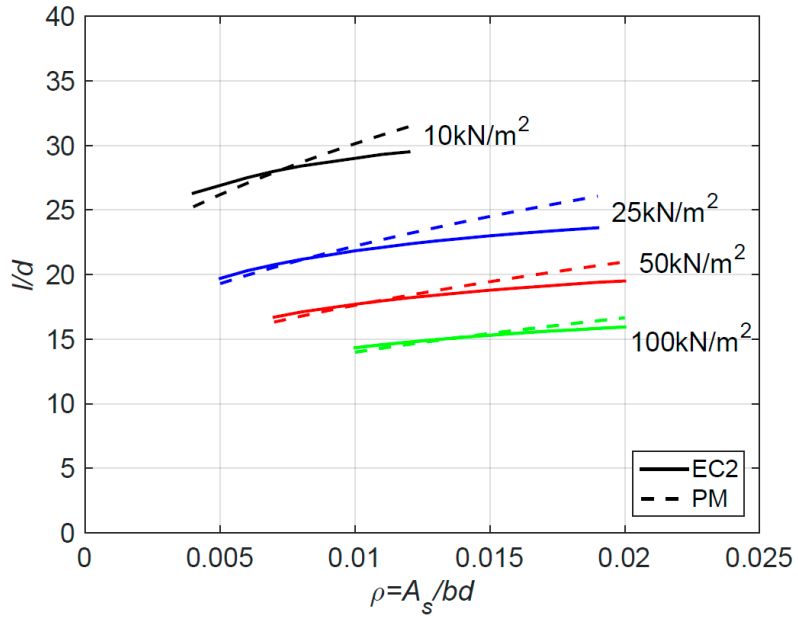

(a)

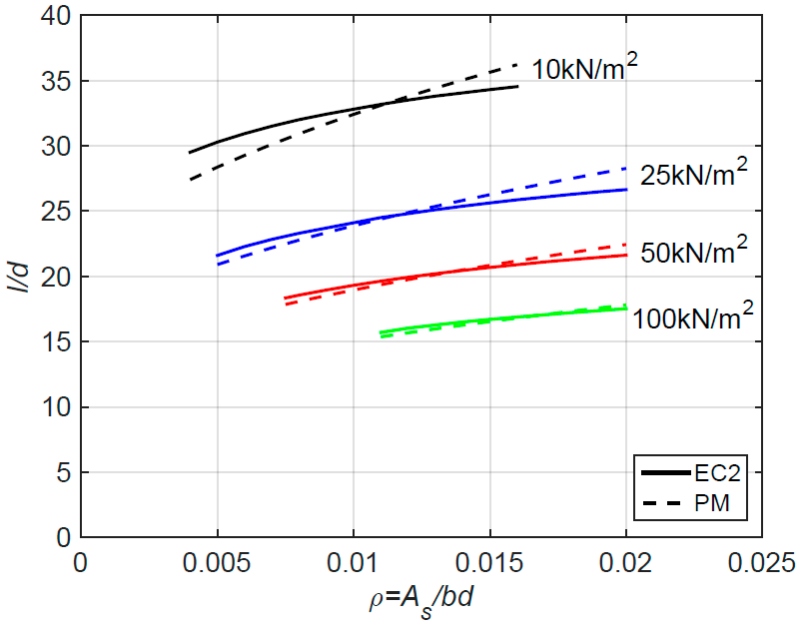

(b)

Figure 15. Comparison between *l/d* values obtained using EC2 [1] and proposed method (PM) for constant load *p/b*=10, 25, 50 and 100 kN/m^2 (a) f_{ck}=30 N/mm^2, (b) f_{ck}=50 N/mm^2.

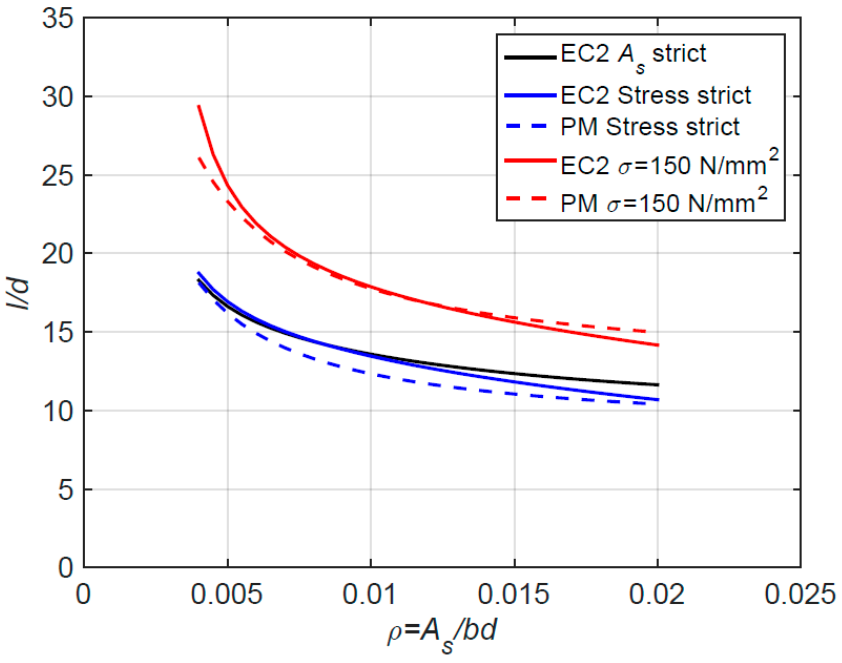

(a)

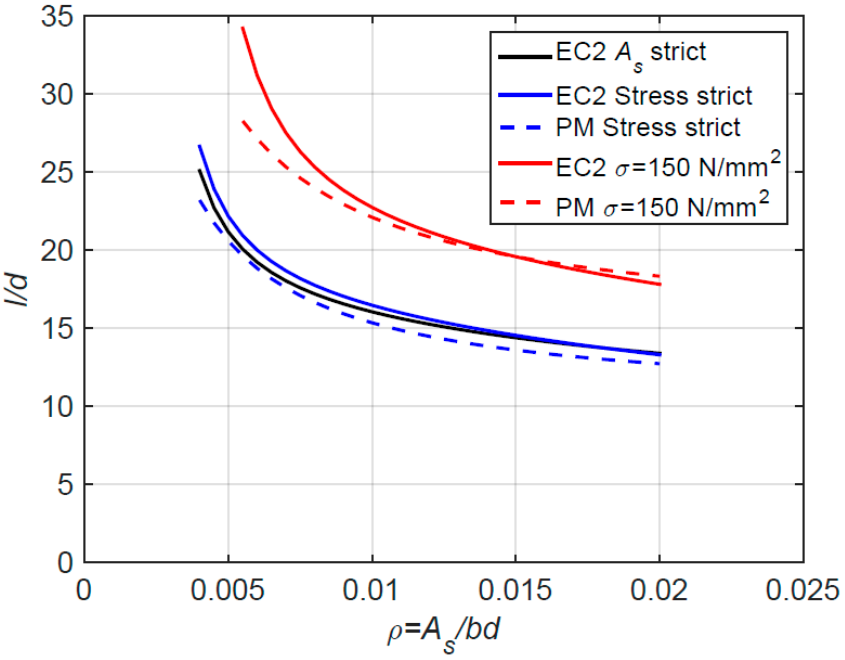

(b)

Figure 16. Comparison between *l/d* values obtained using EC2 [1] and proposed method (PM) for constant stress due to quasi-permanent load (a) f_{ck}=30 N/mm^2, (b) f_{ck}=50 N/mm^2.

885 Table 1. Statistical values of the ratio between *l/d* from proposed method and EC2 [1], for constant

886 *p/b* (Figure 15).

	f_{ck}=30 N/mm^2				f_{ck}=50 N/mm^2			
p_k *(kN/m^2)*	Avg.	Max.	Min.	CoV	Avg.	Max.	Min.	CoV
10	1.01	1.06	0.96	0.036	0.99	1.05	0.93	0.040
25	1.04	1.10	0.98	0.041	1.01	1.06	0.97	0.031
50	1.02	1.08	0.98	0.032	1.00	1.04	0.97	0.022
100	1.01	1.04	0.98	0.023	0.99	1.02	0.98	0.014

887

888 Table 2. Statistical values of the ratio between *l/d* from proposed method and EC2 [1], for constant

889 stress (Figure 16).

	f_{ck}=30 N/mm^2				f_{ck}=50 N/mm^2			
Stress	Avg.	Max.	Min.	CoV	Avg.	Max.	Min.	CoV
150 N/mm^2	1.00	1.06	0.89	0.034	0.98	1.03	0.83	0.048
Strict	0.94	0.97	0.92	0.019	0.94	0.96	0.87	0.016

890